Effect of Structural and Conformation Modifications, Including Backbone Cyclization, of Hydrophilic Hexapeptides on Their Intestinal Permeability and Enzymatic Stability

Shmuel Hess,[†] Oded Ovadia,[†] Deborah E. Shalev,[‡] Hanoch Senderovich,[▽,§] Bashir Qadri,[†] Tamar Yehezkel,[§] Yoseph Salitra,[§] Tania Sheynis,[||] Raz Jelinek,[||] Chaim Gilon,[⊥] and Amnon Hoffman*[,†]

Departments of Pharmaceutics and Organic Chemistry, and the Wolfson Centre for Applied Structural Biology, The Hebrew University of Jerusalem, Safra Campus, Jerusalem 91904, Israel, DeveloGen, Rehovot, Israel, and Department of Chemistry, Ben-Gurion University, Beersheba 84105, Israel

Received July 10, 2007

A library of 18 hexapeptide analogs was synthesized, including sub-libraries of N- or C-methylation of the parent hexapeptide Phe-Gly-Gly-Gly-Gly-Phe, as well as backbone cyclized analogs of each linear analog with various ring sizes. N- or C-methylation as well as cyclization (but not backbone cyclization) have been suggested to improve intestinal permeability and metabolic stability of peptides in general. Here we aimed to assess their applicability to hydrophilic peptides. The intestinal permeability (P_{app}) of the 18-peptide library was in the range of $0.2-6.8 \times 10^{-6}$ cm/sec. Based on several tests, we concluded that the absorption mechanism of all tested analogs is paracellular, regardless of the structural or conformational modifications. In all cases, backbone cyclization increased P_{app} (5-fold) in comparison to the linear analogs due to the smaller 3D size and also dramatically decreased peptide proteolysis by brush border enzymes. N- or C-methylation did not enhance the permeability of the linear analogs in this series.

Introduction

The high selectivity and often unique mode of action of peptides makes them an increasingly important class of potential drugs. However, the poor oral bioavailability limits their usage as therapeutic agents in the clinical setting.[1] This comes from lack of solubility, rapid enzymatic degradation by the intestinal proteolytic enzymes, or poor intestinal permeability. Therefore, there is a substantial need to clearly identify pharmaceutical and chemical approaches that may enhance oral bioavailability of peptides while maintaining their pharmacological activity.

It has been suggested that oral bioavailability of drug candidates can be predicted by the "rule of 5" originally formulated by Lipinski et al.[2] and later revisited by Veber et al.[3] These rules, while valid for most small drug-like molecules, are usually not applicable to peptides, thus, emphasizing the need to reveal the structure−intestinal permeability relationships of these important compounds.

Unlike di- or tripeptides, which are absorbed from the gut by an active transporter, PEPT1, larger peptides are absorbed mainly via passive diffusion due to concentration gradient. This passive permeability across the intestine occurs either via the transcellular pathway (i.e., through the enterocyte membrane) or via the paracellular pathway (i.e., between the enterocyte cells) or via both pathways.

Many of the bioactive peptides are hydrophilic in nature and their site of action is extracellular. For example, many peptides are known (or suspected) G-protein-coupled receptor (GPCR) ligands[4] such that they do not need to penetrate the biological membrane to exert their pharmacologic/physiologic effect. The low membrane permeability of such peptides could indicate that, following oral administration, their intestinal permeability would be limited to the paracellular pathway. This absorption mechanism has been demonstrated for several known peptidic drugs, including octreotide,[5,6] vasopressin,[7] and salmon calcitonin.[8]

While the main features affecting peptide transport via the paracellular route are molecular size, charge, and hydrophobicity,[9] the transcellular route is mainly affected by the energy of desolvation of the solute that controls the entry of the peptide to the hydrophobic interior of the membrane.[10] Conradi et al. have shown that the reduction of the number of potential hydrogen bonds of the peptide backbone through N-methylation leads to a significant improvement in transcellular transport.[10] In addition, Okumu et al. have shown that cyclization of a series of peptides led to improved permeability. This phenomenon could be attributed to enhanced transcellular permeability resulting from elevated lipophilicity and the reduced H-bonding potential characteristic of the cyclic peptides.[11] It has also been suggested that cyclization restricts transcellular permeability of peptides[12] and that several physicochemical properties are dominators of peptide permeability, including LogD, LogP, polar surface area (PSA), and the nonpolar portion of the PSA (NPSA[a]).[13]

Unfortunately, the data currently available on peptide intestinal permeability is limited and is not directly related to the underlying absorption pathway(s). Consequently, rationally designing better orally available peptide drug candidates is hampered.

The purpose of this study was to explore the effect of structural and conformational modifications of hydrophilic peptides on their intestinal permeability and metabolic stability to learn how to improve their oral bioavailability. This was achieved by constructing a library of hexapeptides with the general sequence Phe-Gly-Gly-Gly-Gly-Phe (that contained a

* To whom correspondence should be addressed. Prof. Amnon Hoffman, Department of Pharmaceutics, School of Pharmacy, The Hebrew University of Jerusalem, P. O. Box 12065, Jerusalem 91120, Israel. Tel.: 972 2 6757014. Fax: 972 2 6757246. E-mail: ahoffman@cc.huji.ac.il.

[†] Department of Pharmaceutics.

[‡] Wolfson Centre for Applied Structural Biology.

[§] DeveloGen.

[||] Ben-Gurion University.

[⊥] Department of Organic Chemistry.

[▽] Current address: Predix Pharmaceuticals, Ltd., Ramat Gan, Israel.

[a] Abbreviations: TEER, transepithelial electrical resistance; CR, colorimetric response; NPSA, nonpolar part of the surface area; P_{app}, permeability coefficient; BBMVs, brush border membrane vesicles; PAMPA, parallel artificial membrane permeation assays.

10.1021/jm070836d CCC: $37.00
Published on Web 11/06/2007

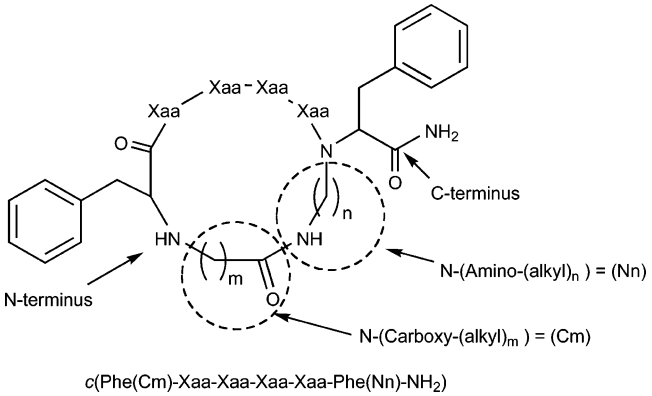

c(Phe(Cm)-Xaa-Xaa-Xaa-Xaa-Phe(Nn)-NH_2)

Figure 1. General structure and nomenclature of the backbone cyclic peptides. Xaa denotes an amino acid (for both backbone cyclic and linear peptides), which can be Gly, Ala, or MeGly. The ring (labeled with two dotted circles) connects two backbone nitrogens, namely, those of the N-terminal and C-terminal Phe residues. The abbreviated name of the cyclic peptide contains the prefix *c* for cyclic and the sequence in parentheses. Cm and Nn (for backbone cyclic and precyclic peptides) represent the number of methylenes in the ring forming arms, m is the number of methylenes in the arm bearing the CO, and n is the number of methylenes in the arm bearing the NH.

positive charge at the N terminus) in which successive Gly → Ala substitutions were made. Additional structural modifications that have been suggested to enhance intestinal stability and permeability were included. Our peptides differed by their topology (i.e., linear versus backbone cyclic), their ring size, and by the number and positions of methyl groups along the peptide backbone (i.e., the degree of N- or C-methylation). Imposing conformational constraints through backbone cyclization allowed us to focus on each structural parameter individually, allowing us to examine its effect on intestinal permeability and metabolic stability.

Backbone cyclization was chosen because it allows cyclization without manipulating the side chains, thus retaining the biological activity of the parent peptide. In backbone cyclization, two amide nitrogens in the peptide are interconnected via a bridge consisting of alkyl groups and an amide or a disulfide bond. Moreover, backbone cyclization combines two structural modifications that were suggested to improve peptide metabolic stability and intestinal permeability, namely, N-alkylation and cyclization[10,11]

Backbone cyclization allows a variety of cyclic structures to be prepared for any given peptide sequence (parent peptide). These can differ in the position, size, and chemistry of the ring.[14] From such a library, a desired biologically active analog can be identified using the appropriate bioassay.

The intestinal permeability characteristics of the hexapeptide libraries were investigated by both in vitro and ex vivo models[15,16] to overcome the possibility of model-dependent results. In addition, the main transport route of the peptides was characterized by screening the permeability across a parallel artificial membrane permeability assay (PAMPA), which consists of a phospholipid vesicle-based barrier.[17,18] In addition, the mechanism was also assessed by comparing the permeability rate following chemically-induced enhancement of tight junction pore size. In addition, we used also a novel approach combining colorimetric and advanced fluorescence spectroscopy techniques, employing probes incorporated within the phospholipid bilayer in lipid/polymer vesicles.[19,20]

No active transport was shown to be involved in the permeability mechanism by comparing the apical to basolateral permeability (A to B) to the basolateral to apical permeability (B to A) for cyclic versus linear peptides in the Caco-2 model.

The stability of the synthesized peptides to enzymatic degradation by intestinal enzymes was determined in enriched brush border membrane vesicles (BBMVs) prepared from rat intestine.[21]

Table 1. (A) Classification of the Peptides into Groups and (B) Structures and Permeability Coefficients (P_{app}) of Peptide Derivatives Investigated in This Study[a]

A

group	chemical modification	peptides
1	ring size	1−4
2	C-methylation (Gly → Ala)	1,5−8
3	N-methylation	1,9−12
4	cyclic vs precyclic vs linear	8,13,14
5	backbone cyclic vs linear	1,6,9,10,15−18

B

peptide	sequence	permeability[b] × 10^6 [cm/sec]	permeability[c] × 10^6 [cm/sec]
Pep1	*c*(Phe(C2)-Gly-Gly-Gly-Gly-Phe(N2)NH_2)	ND[d]	5.43 ± 1.32
Pep2	*c*(Phe(C3)-Gly-Gly-Gly-Gly-Phe(N2) NH_2)	4.2 ± 0.27	2.73 ± 0.79
Pep3	*c*(Phe(C4)-Gly-Gly-Gly-Gly-Phe(N2)-NH_2)	5.02 ± 1.8	1.5 ± 0.5
Pep4	*c*(DPhe(C5)-Gly-Gly-Gly-Gly-Phe(N2)-NH_2)	6.8 ± 1.09	ND[d]
Pep5	*c*(Phe(C2)-Ala-Gly-Gly-Gly-Phe(N2)-NH_2)	3.89 ± 0.51	1.9 ± 0.24
Pep6	*c*(Phe(C2)-Ala-Ala-Gly-Gly-Phe(N2)-NH_2)	5.26 ± 1.79	3.22 ± 0.9
Pep7	*c*(Phe(C2)-Ala-Ala-Ala-Gly-Phe(N2)-NH_2)	6.16 ± 0.52	3.47 ± 1.4
Pep8	*c*(Phe(C2)-Ala-Ala-Ala-Ala-Phe(N2)-NH_2)	5.63 ± 0.75	1.47 ± 0.44
Pep9	*c*(Phe(C2)-MeGly-Gly-Gly-Gly-Phe(N2)-NH_2)	4.58 ± 1.29	2.22 ± 0.57
Pep10	*c*(Phe(C2)-MeGly-MeGly-Gly-Gly-Phe(N2)-NH_2)	3.94 ± 0.77	2.45 ± 1.1
Pep11	*c*(Phe(C2)-MeGly-MeGly-MeGly-Gly-Phe(N2)-NH_2)	5.63 ± 0.75	2.95 ± 0.91
Pep12	*c*(Phe(C2)-MeGly-MeGly-MeGly-MeGly-Phe(N2)-NH_2)	4.87 ± 0.44	1.56 ± 0.26
Pep13	Phe(C2)-Ala-Ala-Ala-Ala-Phe(N2)-NH_2 (precyclic)	0.67 ± 0.1	0.2 ± 0.056
Pep14	MePhe-Ala-Ala-Ala-Ala-MePhe-NH_2	0.56 ± 0.06	0.28 ± 0.02
Pep15	MePhe-Gly-Gly-Gly-Gly-MePhe-NH_2	0.73 ± 0.02	1.82 ± 0.47
Pep16	MePhe-Ala-Ala-Gly-Gly-MePhe-NH_2	0.99 ± 0.33	0.87 ± 0.18
Pep17	MePhe-MeGly-Gly-Gly-Gly-MePhe-NH_2	0.75 ± 0.06	0.58 ± 0.019
Pep18	MePhe-MeGly-MeGly-Gly-Gly-MePhe-NH_2	1.0 ± 0.32	0.46 ± 0.058
mannitol		5 ± 1.1	2.2 ± 0.24

[a] All experiments n ≥ 3 ± SEM. [b] Results obtained from excised tissue. [c] Results obtained from Caco-2. [d] Not determined.

Table 2. Calculated and Found Molecular Mass of the Synthesized Peptides and Their Purity as Determined by HPLC-MS

	calcd mass	found mass	purity %
Pep1	636.4	637.41	93.5
Pep2	650.4	651.36	99.5
Pep3	664.4	665.37	100
Pep4	679.0	679.4	98
Pep5	651.2	650.6	98
Pep6	665.3	664.6	100
Pep7	678.4	678.6	98.3
Pep8	692.5	693.6	100
Pep9	650.4	650.6	100
Pep10	664.0	664.6	100
Pep11	678.0	678.6	93.2
Pep12	691.0	692.6	100
Pep13	693.0	693.4	100
Pep14	623.4	623.4	96
Pep15	567.3	567.6	94
Pep16	595.3	595.5	100
Pep17	581.3	581.7	90
Pep18	595.3	595.7	93

Results

Peptide Design and Synthesis: Three sub-libraries of backbone cyclic hexapeptides with the general sequence *c*(Phe-(Cm)-Xaa−Xaa-Xaa−Xaa-(Nn)Phe-NH_2) and two sub-libraries of linear analogs with the general sequence H-Phe-Xaa-Xaa-Xaa-Xaa-Phe-NH_2 were synthesized to give a total of 18 peptides (see Figure 1 and Table 1a). The molecular weights and product purity of all the synthesized peptides were determined by HPLC-MS and are presented in Table 2.

Peptides 1−4 were designed to investigate the effect of ring size on intestinal permeability (group 1; see Table 1a for the classification of peptides into the different groups). Peptides of groups 2 and 3 were designed and synthesized to study the effect of successive methylation on intestinal permeability. Successive N-methylation of a parent peptide is known to have two effects: it reduces the hydrogen-bonding potential of the peptide and also increases its hydrophobicity. To distinguish between these two effects, a second series of peptides (group 2; peptides 5−8) were synthesized in which successive Gly → Ala substitutions were made. Such substitutions are expected to exert the same effect as N-methylation with respect to the hydrophobicity of the peptide without changing its hydrogen-bonding potential. Thus, by comparing the results obtained for groups 2 and 3, it should be possible to distinguish between effects of hydrophobicity and hydrogen bonding. Group 4 was synthesized to investigate the contribution of backbone cyclization on intestinal permeability compared to linear and precyclic analogs. Group 5 investigated the effect of N-methylation of linear analogs on intestinal permeability.

Ex Vivo Permeability Study: Permeability coefficients (P_{app}) obtained from all the tested peptides are presented in Table 1b. The P_{app} values from group 1 (cyclic ring size effect) show a mean of $5.34 \pm 1.0 \times 10^{-6}$ cm/sec, with no statistically significant difference among the peptides. Groups 2 and 3 (Ala and NMe-Gly substitutions) show P_{app} mean values of $5.06 \pm 0.8 \times 10^{-6}$ cm/sec and $4.75 \pm 0.9 \times 10^{-6}$ cm/sec, respectively, with no statistically significant difference within each group. Peptide 8 (backbone cyclic) in comparison to peptide 13 (precyclic) and peptide 14 (linear) have P_{app} values of 5.63 ± 0.8, 0.67 ± 0.1, and $0.56 \pm 0.1 \times 10^{-6}$ cm/sec, respectively, $p < 0.01$ (see Figures 2 and 4). Group 5 (linear analogs differing by degree of N-methylation) has a P_{app} mean of $0.91 \pm 0.1 \times 10^{-6}$ cm/sec, with no statistical significance among the peptides, Figure 2.

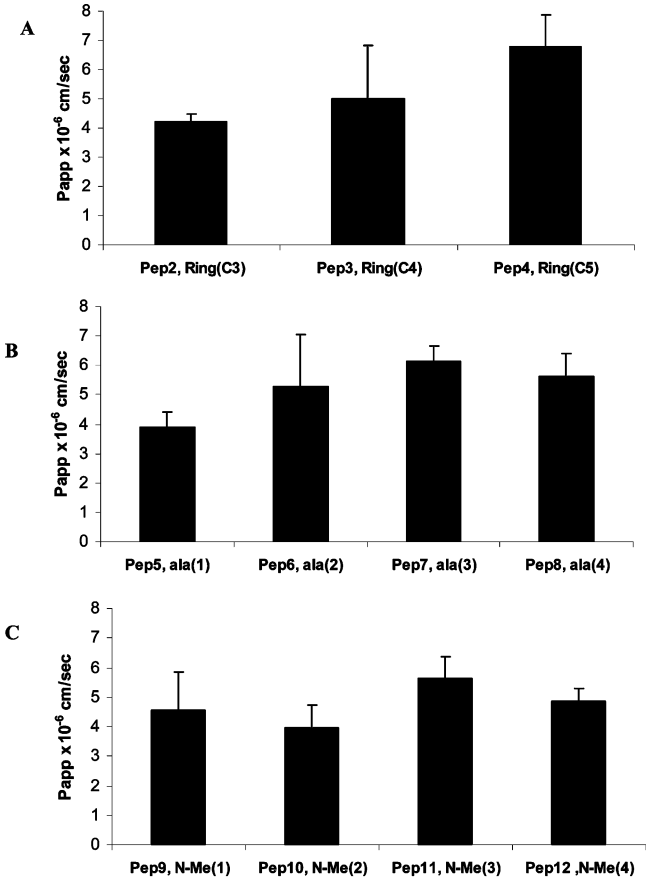

Figure 2. Side-by-side diffusion chamber: Effect of the cyclic ring size on intestinal permeability (A); effect of the degree of Ala content on backbone cyclic permeability (B); effect of the degree of N-methylation on cyclic peptide analogs (C); all experiments, $n \geq 3 \pm$ SEM.

In Vitro Caco-2 Permeability: P_{app} values of all tested peptides are presented in Table 1b. P_{app} values obtained from group 1 (backbone cyclic ring size effect) show a P_{app} of $3.71 \pm 0.4 \times 10^{-6}$ cm/sec, with no statistically significant difference among the peptides. Groups 2 and 3 (Ala and NMe-Gly substitutions) show a mean P_{app} of $2.7 \pm 0.8 \times 10^{-6}$ cm/sec and $2.3 \pm 0.8 \times 10^{-6}$ cm/sec, respectively, with no significant difference within the groups. The peptides in group 4 (except peptide 15) show a mean P_{app} of $0.48 \pm 0.1 \times 10^{-6}$ cm/sec with no significant difference within the group, Figure 3. It, thus, should be noted that there were significant differences beween the permeability rate constant for the cyclic derivatives in comparison to the noncyclic peptides (Figures 2 and 4).

Assessment of the Intestinal Permeability Mechanism: There are several methods to evaluate the mechanism of transport via the intestinal wall. Based on our hypothesis that the current transport mechanism is predominantly the paracellular pathway, we chose to study their transport mechanism via several independent methods.

The first method used was to enhance the paracellular route by using palmitoyl carnitine,[9] a specific modulator of the tight junctions in the Caco-2 monolayer. We observed enhanced transport rates of mannitol (240% in the P_{app} value), as well as the permeability of two selected representative peptides, peptide 9 and its linear counterpart, peptide 17. The P_{app} values of peptides 9 and 17 were raised from 2.2 to 7.58×10^{-6} cm/sec (340%) and from 0.58 to 1.74×10^{-6} cm/sec (340%), respectively, Figure 5.

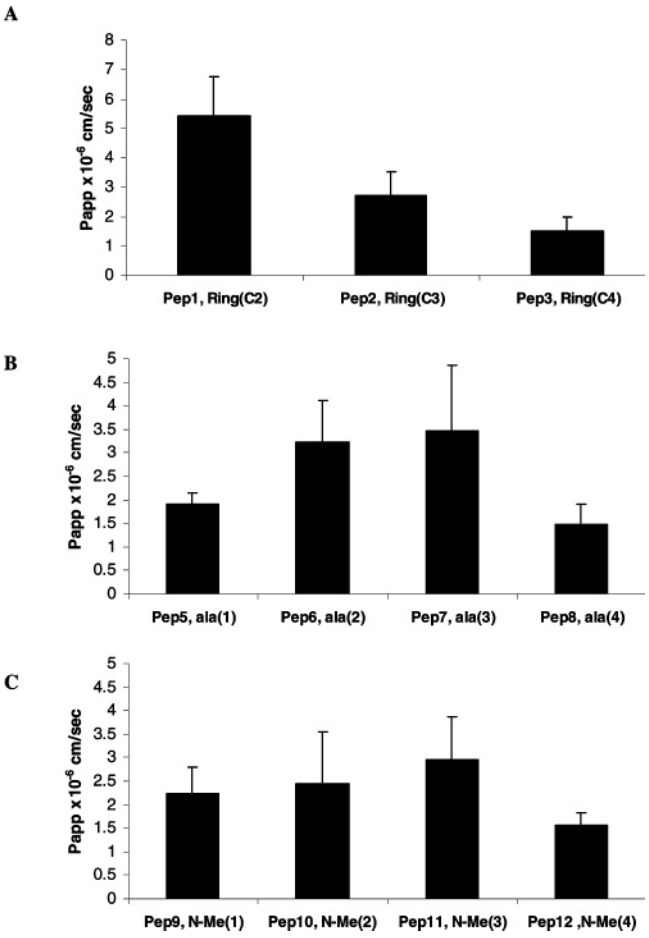

Figure 3. Caco-2 cell culture model: Effect of the cyclic ring size on intestinal permeability (A); effect of the degree of Ala content on backbone cyclic permeability (B); effect of the degree of N-methylation on cyclic peptide analogs (C); all experiments, $n \geq 3 \pm$ SEM.

The second method is a novel colorimetric mixed-vesicle assay that evaluates whether the peptides have any interaction with a bilayer membrane. The colorimetric platform comprises an aqueous solution of mixed bilayer vesicles containing phospholipids [such as dimyristoylphosphatidylcholine (DMPC), used herein] and polydiacetylene (PDA), as described before by Kolusheva et al.[20] Specifically, the DMPC domains interspersed within the PDA matrix serve as the biomimetic membrane layer, while the polymer acts as a colorimetric reporter. When the test compound interacts with the bilayer membrane, it causes structural alterations of the pendant side chains of the polymer at the vesicle interface that are expressed by a change in color from blue to red as well as a modification of the fluorescence quenching. The results are depicted in Figure 6 in comparison to cyclosporine, which served as a marker for transcellular transport. Cyclosporine had a 25% blue to red transition, whereas peptides 1 (backbone cyclic), 15 (linear), 9 (backbone cyclic), and 17 (linear) had no effect on color transition, Figure 6A. Fluorescence quenching was assessed with DMPC/NBD-PE tests that showed a 62% decrease in fluorescence with cyclosporine compared to a 40% decrease of peptides 1 and 15 (cyclic versus linear). Peptides 9 and 17 (cyclic versus linear) showed a decrease of 35%, a result similar to the control (quencher alone), Figure 6B.

To further validate the results obtained from this novel method, peptide permeability was studied with an artificial membrane using the established method, $PAMPA_{lecithin}$.

None of the peptides tested by $PAMPA_{lecithin}$ permeated the phospholipid bilayer. Testosterone and antipyrine, serving as transcellular markers, were found to permeate the barrier, while paracellular markers such as mannitol and amoxicillin did not permeate the artificial membrane (Table 3). The permeability through Caco-2 cells of representative peptides 9 and 17 was evaluated from basolateral to apical (Figure 7) to ensure that no active transporters are involved in absorbing the tested peptides. The results clearly demonstrate that the transport rate of these peptides from apical to basolateral (A to B) is similar to the B to A transport rate.

Metabolic Stability: The metabolic stabilities of the backbone cyclic peptides and their linear analogs were studied in BBMVs, which are known to have broad enzymatic degradation activity, and were compared to an enzyme-free buffer (MES 50 mM, pH 7.4). Two cyclic peptides, 1 and 8, and two linear peptides, 14 and 13 (precyclic), were tested. The cyclic analogs showed significant resistance to metabolic degradation after 90 min in BBMVs (100% recovery) in comparison to the fast and significant decay of the linear analogs (30% recovery) under the same experimental conditions, Figure 8.

Physiochemical Properties: Experimental (LogD $pH_{7.4}$)-values and calculated PSA of the backbone cyclic peptides and their linear analogs are presented in Table 4. No correlation was found between the P_{app}s and these physiochemical properties.

Furthermore, considering the importance of the hydrodynamic volume when macromolecules pass through a narrow pore, that is, in the paracellular route, we experimentally studied the effective size of the molecule and its impact on restricted pore size permeability. We choose high-resolution size exclusion chromatograph as a model.

The capacity factor, K', was determined for the peptides by high-resolution size exclusion chromatography. As depicted in Table 5, the backbone cyclic peptides were found to have a smaller molecular hydrodynamic volume than their linear and precyclic analogs.

NMR Studies: Nuclear magnetic resonance measurements were performed on three representative peptides from the different groups; 1 and 2 as representative cyclic peptides and 15 as a linear control. Both cyclic peptides showed two conformations with a ratio of approximately 1:0.2 at 25 °C in both water and DMSO. The conformations showed pairs of amide interactions in the TOCSY spectra,[22] indicating structural exchange on the time scale of the NMR measurement. Further temperature-dependence experiments on the cyclic peptides, ranging between 25 and 40 °C, also indicated a change in the ratio of the amide peaks from 1:0.2 to 1:0.4. The two conformations of the linear peptide were evident but unresolved, apart from one glycine, presumably Gly5 adjacent to the N-methyl Phe6 at the carboxy terminus, which can have both *cis*- and *trans*-conformations.

No structural information could be determined from the NOESY or ROESY spectra,[23] which gave no interactions apart from those expected due to covalent bonds. This is most likely due to the size of the ring and the fact that the glycine residues can give no side chain-to-backbone or side chain-to-side chain interactions. This left us with ambiguously assigned spectra, although the residue identity of the peaks was made (Table 6).

Discussion

There is a wide range of bioactive peptides that are hydrophilic in nature. In most cases their site of action is on the outer surface of cells (e.g., GPCR receptor ligands) that do not require

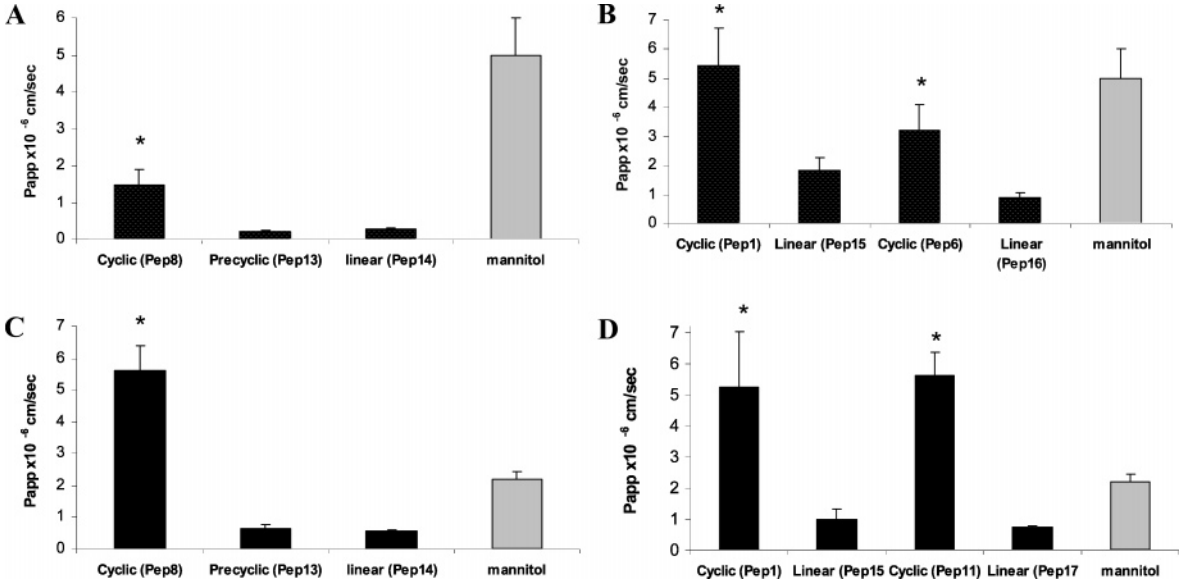

Figure 4. Permeability coefficients of backbone cyclic peptides compared to precyclic and linear analogs in the Caco-2 model (A); permeability coefficients of backbone cyclic peptides compared to additional linear analogs in the caco-2 model (B); permeability coefficients of backbone cyclic peptides compared to precyclic and linear analogs in the side-by-side diffusion chamber (C); permeability coefficients of backbone cyclic peptides compared to additional linear analogs in the side-by-side diffusion chamber (D); all experiments $n \geq 3 \pm$ SEM. *Statistical difference between cyclic, precyclic, and linear analog, $P < 0.05$.

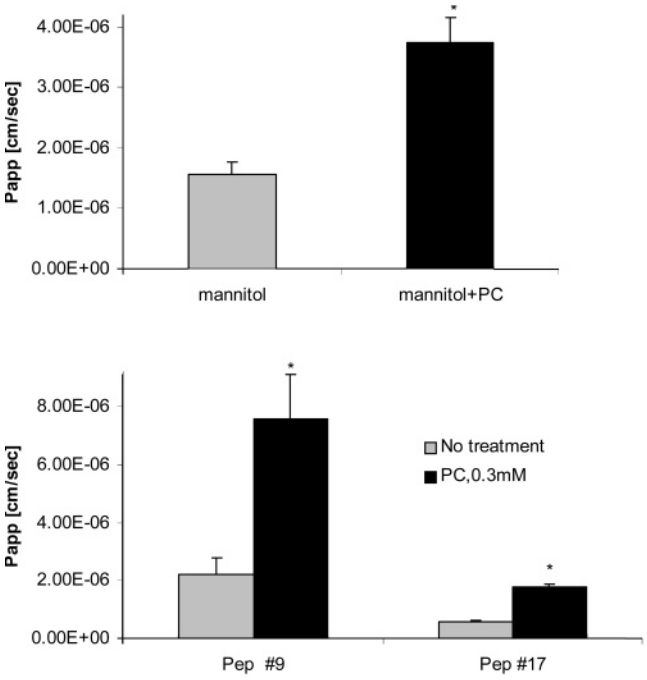

Figure 5. Effect of paracellular transport enhancer (palmitoyl carnitine) on the permeability of mannitol, peptide 9 and its linear analog, and peptide 17 in the Caco-2 model; $n \geq 3 \pm$ SEM. *Statistical difference compared to the nontreated cells, $P < 0.05$.

membrane permeability. In general, high intestinal permeability leading to enhanced oral bioavailability is desired for developing peptide-based drugs. While lipophilic compounds tend to permeate the cell membrane by the transcellular mechanism and to yield high intestinal absorption characteristics (e.g., cyclosporine), hydrophilic compounds are transported through biological membranes via active transporters or by passive diffusion via paracellular pathways. To date, the mechanism of membrane permeability of the peptides was not investigated when structure−permeability relationships were studied, despite the meaningful implications of this information. In this work we focused on investigating the transport mechanism(s) of hydrophilic hexapeptides and the possible effect of certain structural modifications. The structural and conformational modifications that we tested were previously suggested in the literature to improve membrane permeability and could, in theory, convert the absorption mechanism (at least in part) from the paracellular to the transcellular pathway. Our working hypothesis was that the hydrophilic hexapeptide analogs investigated in this work would permeate the intestine only by the paracellular pathway.

The main finding of this work is that the structural modifications that were originally suggested to improve intestinal permeability of peptides were found not to affect the intestinal permeability of the investigated hexapeptides, except for the impact of backbone cyclization that will be detailed below. Specifically, the degree of N-methylation in our study was consistent (i.e., for both backbone cyclic and linear peptides) and found not to affect permeability by hexapeptides. This finding is unique in light of previous reports suggesting N-methylation as a structural modification that improves permeability due to the reduced H-bond potential, thus improving the ability of the peptide to traverse the transcellular pathway. Moreover, increasing the peptide methyl content (through Gly → Ala modifications), and thereby increasing lipophilicity, did not improve permeability. This fact is consistent with our hypothesis that the tested hexapeptides were predominantly transported via the paracellular pathway, which is not expected to be enhanced by increased lipophilicity. The P_{app} values obtained from the Caco-2 model (Figure 3) were lower than those obtained in the diffusion cell model (Figure 2), further corroborating our hypothesis. These findings are in accord with the known differences in the tight junction pore size between the two models.[24] We used $PAMPA_{lecithin}$ to further verify the hypothesis that the permeability occurs predominantly via the tight junction space. This artificial membrane screens for molecules that tend to permeate by the passive transcellular mechanism. The negligible permeability of the tested peptides through the $PAMPA_{lecithin}$ also confirms the hypothesis of predominate paracellular rather than transcellular transport.

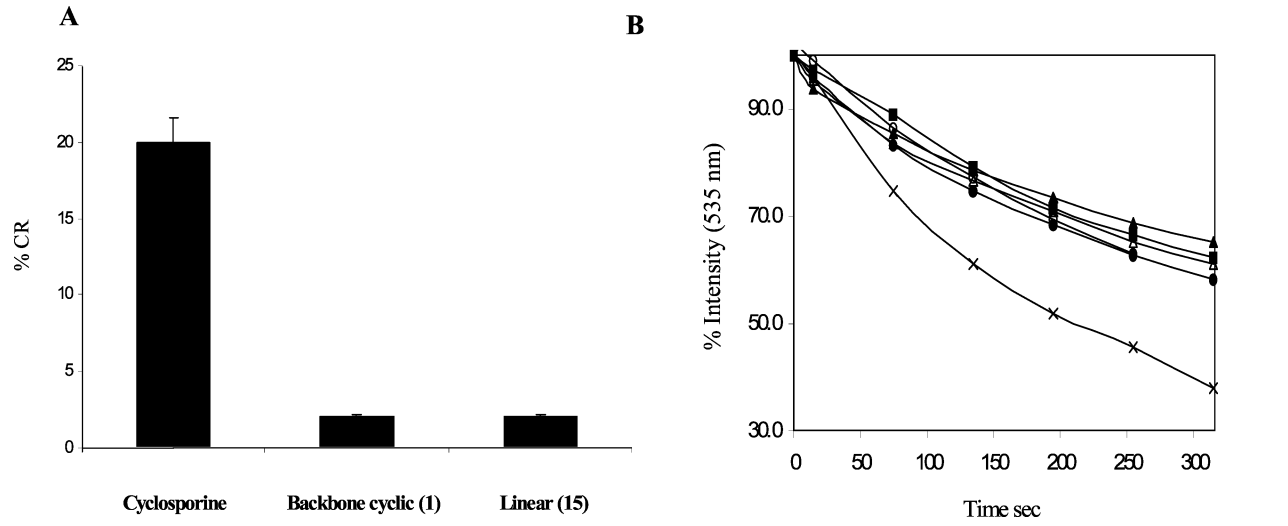

Figure 6. Colorimetric transitions induced by peptides in DMPC vesicles. The percentage of colorimetric response (%CR, see Experimental Section) induced by tested peptides and cyclosporine as a positive control (A). Time-resolved fluorescence quenching of NBD-PE. Decay of the fluorescence (5358 nM) of NBD-PE dye induced by sodium dithionite-induced quenching of fluorescence emission after adding peptides relative to the control (no peptides added; □) control; (●) cyclic analog peptide 1; (■) cyclic analog peptide 9; (▲) linear analog peptide 15; (◇) linear analog peptide 17; (×) cyclosporine A, (B). All peptides were added at a concentration of 30 μM.

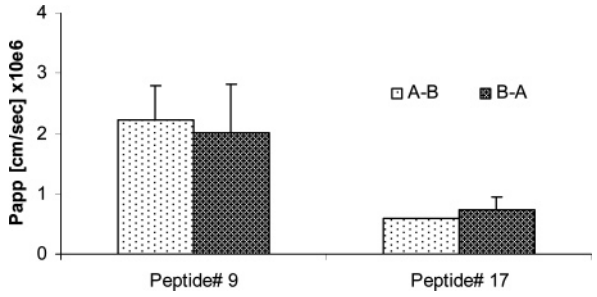

Figure 7. Permeability coefficients of backbone cyclic peptide (Pep9) and its linear counterpart (Pep17) in apical to basolateral (A-B) and basolateral to apical (B-A) in Caco-2 cells; $n \geq 3 \pm$ SEM.

Table 3. Permeability of Members of the Library Peptides in the PAMPA Model in Comparison to That of the Transcellular and Paracellular Markers

cmpd	Pe × 10^6
testosterone	8.67 ± 4.06
antipyrine	1.18 ± 0.39
acyclovir	0.01 ± 0.001
mannitol	ND[a]
amoxycilin	ND
peptide 3	ND
peptide 7	ND
peptide 8	ND
peptide 9	ND
peptide 12	ND
peptide 14	ND
peptide 17	ND

[a] ND: not detected.

Palmitoyl carnitine, which increases permeability via the paracellular route, enhanced permeability of peptides 9 and 17, similar to the effect seen for mannitol (Figure 5).

A novel colorimetric assay was used to assess whether the peptides tend to interact with a bilayer membrane of the lyposomes.[19] The results (Figure 6) suggest that both the backbone cyclic peptides studied in this work and their linear analogs do not interact with the liposome membrane, indicating that they are also unable to penetrate through the model bilayer and are supporting a predominately paracellular rather than transcellular transport.

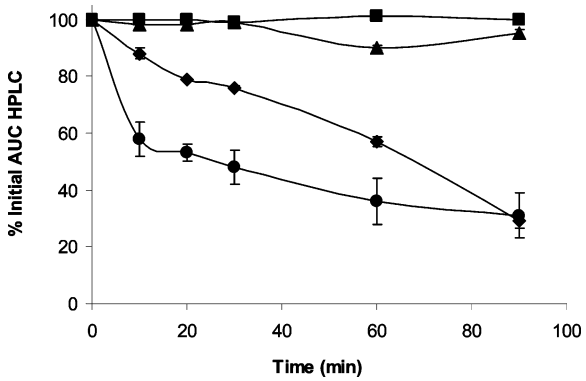

Figure 8. Metabolic stability in brush border membrane vesicles (BBMVs), (●) linear analog, peptide 14; (◆) precyclic analog, peptide 13; (▲) backbone cyclic analog, peptide 8; (■) backbone cyclic analog, peptide 1; $n \geq 3 \pm$ SD.

Table 4. Comparison of Cyclic (1, 8, 9) and Linear (15, 14, 17) Physiochemical Properties

peptide	$LogD_{octanol/7.4}$[a]	PSA Å	PSA\NPSA
Pep1	−0.41	195	0.35
Pep15	ND[b]	137	0.22
Pep8	0.49	144	0.19
Pep14	ND	181	0.3
Pep9	−0.57	172	0.28
Pep17	ND	154	0.25

[a] Determined by the shake-flask method in octanol/buffer pH 7.4. [b] ND: not determined.

Table 5. Capacity Factors (K′) Obtained by Size Exclusion Chromatography, Indicating the Relative Molecular Size of Backbone Cyclic Peptides Compared to Their Linear and Precyclic Analogs

peptide	K′
Pep8	0.75
Pep13	0.6
Pep14	0.45

The similar permeability rates observed for the A to B and B to A (Figure 7) indicate there are no active transport processes (i.e., influx/efflux) involved in the permeation process of the peptides. Thus, the only driving force for permeation is diffusion due to the concentration gradient.

Table 6. Proton Chemical Shifts of the Major Conformations of Cyclic (2) and Linear (15) Peptides in 10% D_2O in Water at 25 °C

residue identity	HN protons	α protons	β protons	others (ppm)
		Peptide 15 NMePhe-Gly-Gly-Gly-Gly-NMePhe		
Phe		5.13	3.29, 3.01	aromatics 7.21−7.40,
Phe		4.72	3.30, 2.98	methyls 2.68, 2.84
Gly	8.65	3.91		
Gly	8.38	3.94		
Gly	8.12	3.93		
Gly	8.00	4.01, 3.84		
NH_2				amides 7.10, 7.52
		Peptide 2 *c*(Phe(C3)-Gly-Gly-Gly-Gly-Phe(N2) NH_2)		
Phe		4.60	3.11, 3.19	7.19, 7.30, 7.48
Phe		4.06	3.29, 3.08	
Gly	8.53	3.88, 4.03		
Gly	8.19	3.83, 4.00		
Gly	8.12	3.89, 4.16		
Gly	7.89	2.97, 4.06		
C3 bridge arm				3.03, 2.98, 2.32, 1.98, 1.79
N2 bridge arm	6.89			3.39, 3.22, 2.98, 2.88
NH_2				amides 7.01, 7.50

Taken together, the results obtained in this study substantially verify the hypothesis that the molecular compositions of the studied hexapeptides direct the transport mechanism toward the paracellular pathway.

Although the paracellular area is relatively small compared to the transcellular area, 0.01%[25] to 0.1%,[26] the intestinal epithelium has a surface area of over 2×10^6 cm^2,[27] while the corresponding values of the paracellular surface ranges from 200 to 2000 cm^2.[28] This surface area should not be underestimated because even the absorption of minute quantities (pM−nM) of a peptide drug may be sufficient to exert its required pharmacological effect due to the high potency of bioactive peptides. Several peptide drugs such as octreotide, vasopressin analogs, and desmopressin are believed to be absorbed by this route.[29]

The improved intestinal permeability of the backbone cyclic peptides via the paracellular route is of interest in view of previous reports, suggesting that cyclization enhances peptide permeability by shifting it toward transcellular transport.[11] The improved permeability via the inter-enterocyte space obtained by cyclization (as demonstrated in Figures 2−4) can be explained by the conformational constraint imposed, which results in a much more constrained three-dimensional geometry. This constrained conformation is seen in the distribution of molecular conformations computed by molecular dynamic simulations. The backbone cyclic peptides spent 99% of the time in a single conformation, whereas their linear analogs span a much broader conformational space, significantly populating several conformations.

The NMR studies that were carried out in the attempt to define three-dimensional conformations were not sufficiently resolved for this purpose. The fact that backbone cyclization imposes a more strict conformation and, therefore, a smaller molecular volume can be shown empirically by a molecular size study utilizing high-resolution peptide size exclusion chromatography and is also evident in the resolved α protons of the glycines and bridge methylenes relative to the linear analogs (Table 6). High-resolution peptide size exclusion chromatography enables discrimination among peptides based on size (i.e., larger peptides are associated with a shorter retention time indicated by a smaller capacity ratio). As shown in the results (Table 5), higher capacity ratios (K') were found for the cyclic peptides compared to linear and precyclic analogs. This indicates a reduced conformational space of the cyclic peptide as compared to that of the precyclic and linear analogs. Reduced dimensions induced by increased conformational constraints contributes to enhanced paracellular transport, as shown in the "sieving theory" proposed by Watson et al.[30] This theory suggests that hydrodynamic volume and conformation are the main factors dominating paracellular transport. The transport of a molecule across the paracellular path contains two components combining restrictive and nonrestrictive pores, where the restrictive path serves as a sharp molecular size cutoff and the nonrestrictive path for this size of molecules provides transport for larger molecules.

Enzymatic stability of peptides in the gut lumen and the brush border is a major factor dominating the oral bioavailability of peptides, as these regions are abundant with proteolytic enzymes that considerably reduce the ability of intact peptides to reach the systemic circulation following intraintestinal administration. For tetra- and higher peptides, over 90% of the proteolytic activity is in the brush border membrane, whereas for tripeptides it is 10−60% and for dipeptides it is only 10%.[31] Our results comparing the metabolic stability of backbone cyclic, precyclic, and linear hexa-peptides in the brush border membrane vesicle model (Figure 8) show that cyclization of peptides significantly increases their stability toward degradation by peptidase enzymes that are bound to the brush border membrane. This is probably due to the drastic decrease in the ability of the peptide to attain the linear, flexible conformation necessary for its interaction with the catalytic site of the proteolytic enzymes.[32] These results are in agreement with previous reports in our laboratory demonstrating significant metabolic stability of backbone cyclic peptides in various media such as serum and kidney homogenate.[33,34] It should be noted that the peptides are exposed to the brush border enzymes regardless of the permeability pathway. Thus, the peptides investigated in this study could be available for brush border degradation regardless of the mechanism of transport.

Conclusion

This study presents a systematic investigation into the effect of various factors previously suggested to affect peptide intestinal permeability and stability. We conclude that backbone cyclization significantly improves paracellular intestinal permeability and stability compared to that of linear analogs. Structural modifications that have been suggested to affect peptide intestinal permeability (e.g., N-methylation) do not seem to have a significant influence when the transport mechanism is paracellular. The current investigation highlights that, when per-

meating the intestinal wall via the paracellular pathway, conformational rigidity and molecular space (e.g., hydrodynamic volume) play the most important role in intestinal permeability.

Experimental Section

Chemicals: Unless otherwise specified, all reagents and chemicals were purchased from Sigma-Aldrich (St. Louis, MO). HPLC grade water, methanol, and acetonitrile were purchased from J. T. Baker (Holland).

Animals: Male Sabra rats weighing 250−300 g were used for the ex vivo permeability study. The project adhered to the principles of Laboratory Animal Care (NIH publication no. 85−23, revised 1985). All animals were deprived of food but not water 12 h prior to the experiments.

Peptide Synthesis: Backbone cyclic analogs tested in this study were synthesized by solid phase, multiple parallel synthesis, using Fmoc chemistry as previously described,[35] which was adapted to a 96-well format. Syntheses were performed on an ACT 396 synthesizer (Advanced ChemTech, Louisville, KY) equipped with a Lab Tech 4 (Advanced ChemTech, Louisville, KY) for heating. The backbone cyclic building units were protected on their ω-carboxy or ω-amine by the allyl/alloc protecting group, which was removed before on resin cyclization. The synthesis scale was 6 μmol Rink amide MBHA resin, which resulted in approximately 5 mg of crude product/well. Amino acid coupling to MBHA−resin or to peptidyl−resin was carried out with Fmoc-protected amino acid (5 equiv excess to resin) preactivated for 10 min with HBTU/HOBT (5 equiv) and diisopropylethyl amine (10 equiv) in *N*-methylpyrolidinone at room temperature. Coupling to the *N*-alkylated amino acid moieties of the peptidyl−resin was performed according to Falb et al.[36] Briefly, Fmoc amino acid and bistrichloromethylcarbonate were dissolved in dioaxane or 1,3-dichloropropane, cooled in ice water, and collidine was added carefully. The mixture was added to the resin and heated to 50 °C for 1 h. After washing, the Fmoc group was removed by 25% piperidine in *N*-methylpyrolidinone for 20 min (×2). At the end of the assembly, allyl/alloc deprotection on the bridging arms was performed with tetrakis (triphenylphosphine)-palladium(0). Cyclization was performed on the resin using benzotriazole-1-yl-oxy-tris-pyrrolidinophosphonium hexafluorophosphate. Cleavage from the resin was carried out by a reagent mixture (92.5% trifluoroacetic acid, 2.5% triisopropyl silane, and 2.5% ethane dithiol, 1 h). The crude peptides were partially purified by C_{18} Sep-Pak chromatography using 50% acetonitrile in water as the eluent. The molecular weight and purity of the peptides was determined by LC-MS using Waters Millenium LC-MS instrument equipped with Micromass ZQ detector, Waters 600 Controller gradient pump, and Waters 717 auto-sampler. The analysis was conducted using Xterra MS C18 column 2.1 × 150 mm (Table 2). Large scale synthesis was carried out according to procedures described previously.[37]

Ex Vivo Animal Permeability Study: Permeability experiments were performed in a modified Ussing chamber system (Physiological Instruments, Inc., San Diego, CA). Following a midline incision to the rat, 25 cm of small intestine was removed and placed in ice-cold Ringer bicarbonate buffer (NaCl 6.54 g, KCl 0.37 g, $CaCl_2 \times 2H_2O$ 0.18g, $MgCl_2 \times 6H_2O$ 0.24 g, $NaHCO_3$ 2.1 g, Na_2HPO_4 0.23 g, NaH_2PO_4 0.05g in 1000 mL). All buffer solutions were freshly prepared and equilibrated to pH 7.4, osmolality 290 mOsm. The jejunal portion of the small intestine (10−15 cm distal to the pylorus) was used. Peyer patches could be easily identified visually, and sections containing them were not used in these studies. The individual segments were obtained, and underlying muscularis was removed from the serosal side of the tissue before mounting. The exposed tissue surface area was 0.5 cm^2 and fluid volume in each half-cell was 5 mL. The system was preheated to 37 °C. Modified Ringer buffers were added to the serosal and the mucosal sides (mucosal modified Ringer buffer contained 10 mM mannitol and serosal modified Ringer buffer contained 8 mM D-glucose and 2 mM mannitol). The tissue oxygenation and the solution mixing were performed by bubbling with 95% O_2−5% CO_2. The system was equilibrated for 30 min. The permeability experiments continued for 180 min and samples were withdrawn at predetermined times. The sampled volume was replaced by blank (noncompound containing) buffer to maintain sink conditions. The integrity of the epithelial tissue was monitored by measuring the transepithelial electrical resistance (TEER) throughout the experiment. Viability was assessed by applying 1 μM forskolin at the end point (180 min), and an increase or decrease of above 5% in Isc was observed. Any tissue with values <30 Ωcm^2 was discarded before the start of the experiment. Generally, TEER values were 70−130 Ωcm^2 and remained steady throughout the experiment.

In Vitro Permeability Study. Growth and Maintenance of Cells: Caco-2 cells were obtained from ATCC and then grown in 75 cm^2 flasks with approximately 0.5×10^6 cells/flask at 37 °C in 5% CO_2 atmosphere and at a relative humidity of 95%. The culture growth medium consisted of Dulbecco's modified Eagle medium supplemented with 10% heat-inactivated fetal bovine serum, 1% nonessential amino acids, and 2 mM L-glutamine. The medium was replaced twice weekly.

Preparation of Cells for Transport Studies: For the transport studies, cells in a passage range of 60−66 were seeded at a density of 25×10^5 cells/cm^2 on untreated culture inserts of polycarbonate membrane with 0.4 μM pores and surface area of 1.1 cm^2. The culture inserts containing Caco-2 monolayer were placed in 24 transwell plates, 12 mm, Costar. The culture medium was changed every other day. Transport studies were performed 21−23 days after seeding, when the cells were fully differentiated and the TEER values were stable (300−500 $\Omega \times cm^2$).

Experiment Protocol: Transport study (apical to basolateral, A to B) was initiated by removing the medium from both sides of the monolayer and replacing it with apical buffer (550 μL) and basolateral buffer (1200 μL), both warmed to 37 °C. The cells were incubated for 30 min at 37 °C with shaking (100 cycles/min). After the incubation period, the buffers were removed and replaced with 1200 μL of basolateral buffer on the basolateral side. Test solutions were warmed previously to 37 °C and added (600 μL) to the apical side of the monolayer. Samples (50 μL) were taken from the apical side immediately at the beginning of the experiment, leaving a 550 μL apical volume during the experiment. For the period of the experiment, the cells were kept at 37 °C with shaking. At predetermined times (30, 60, 90, 120, 150, and 180 min), 200 μL samples were taken from the basolateral side and replaced with the same volume of fresh basolateral buffer to maintain a constant volume.

For the basolateral to apical study (B to A), compounds were placed in the basolateral chamber, followed by sampling the apical side similar to the A to B protocol.

Physiochemical Properties. Lipophilicity: Log $D_{oct/7.4}$ shake-flask was determined by the shake-flask method. Octanol and MOPS buffer were presaturated prior to the experiment. The vials were shaken overnight in a Vortex Genie 2 (Freid, Israel). Both phases (octanol and MOPS buffer) were analyzed by HPLC. The final $D_{oct/7.4}$ value was calculated by dividing the areas corresponding to the compound in the two phases ($D = A_{octanol}/A_{buffer}$), while A corresponds to the area of the peak.

Molecular Size: The average hydrodynamic volumes of the backbone cyclic peptides and their linear analogs were estimated by high-resolution size exclusion chromatography performed in 0.02 M phosphate buffer, pH 7.4, with 0.25 M NaCl using a superdex peptide 30/100 HR column (10 × 100 mm, Pharmacia Biotech, Uppsala, Sweden). The peptide solution (50 μL, ~1 mg/mL, in running buffer) was injected on the column and solutes were detected with a UV detector at $\lambda = 254$ nm.

Data Analysis: Permeability Coefficient (P_{app}): The P_{app} for each compound was calculated from the linear plot of drug accumulated versus time, using the following equation

$$P_{app} = 1/(C_0 \times A) \times dQ/dt$$

where dQ/dt is steady state appearance rate of the drug on the receiver side, C_0 is the initial concentration of the drug on the donor

side, and A is the exposed tissue surface area, 0.5 cm^2 tissue area and 1 cm^2 in the Caco-2 experiments.

Interaction with the Liposome Bilayer. Vesicle Preparation: All lipid constituents were dissolved in chloroform/ethanol (1:1, v/v) and dried in vacuo to a constant weight. All lipids were suspended in deionized water, followed by probe sonication on a Misonix Incorporated sonicator (Farmingdale, NY), applying an output power of ~100 W. Vesicles containing lipid components and PDA were sonicated at 70 °C for 3−4 min. The vesicle suspensions were then cooled to room temperature, incubated overnight at 4 °C, and polymerized by irradiation at 254 nm for 20−30 s, resulting in solutions with an intense blue color. Vesicle suspensions were allowed to anneal for 30 min and centrifuged for 15 min at 6000 *g* to remove titanium particles.

UV−vis Measurements: Peptides at a concentration of 30 μM were added to 60 μL of polydiacetylene (PDA) containing vesicle solutions consisting of ~0.2 M phospholipids in 25 mM Tris-base (pH 8.0). Following addition of the peptides, the solutions were diluted to 1 mL and spectra were acquired at 28 °C, between 400 and 700 nm, on a Jasco V-550 spectrophotometer (Jasco Corp., Tokyo, Japan), using a 1 cm optical path cell.

To quantify the extent of blue-to-red color transitions within the vesicle solutions, the percentage colorimetric response (%CR) was defined and calculated as follows

$$\%CR = (PB_0 - PB_I/PB_0) \times 100$$

where $PB = A_{blue}/(A_{blue} + A_{red})$ and A is the absorbance at 640 nm (the "blue" component) or 500 nm (the "red" component). The colors "blue" and "red" refer to the visual appearance of the material, not the actual absorbance. PB_0 is the blue/red absorption ratio of the control sample before the induction of a color change and PB_I is the value obtained for the vesicle solution after the colorimetric transition occurred.

Fluorescence Quenching Measurements: NBD-PE was added to lipids from a 1 mM chloroform stock solution, yielding a final concentration of 4 μM, and then dried together by vacuum sonication (see Vesicle Preparation). Samples were prepared by adding peptides, at a bound concentration of 30 μM, to 60 μL of vesicle solutions at ~0.2 mM total lipid concentration in 25 nm Tris-base (pH 8.0). The quenching reaction was initiated by adding sodium dithionite from a 0.6 M solution, prepared in 50 mM Tris base (pH 11.0) buffer, to a final concentration of 0.6 mM. The decrease in fluorescence was recorded for 210 s at 28 °C using 468 nm excitation and 538 nm emissions on an Edinburgh FL920 spectrofluorimeter. The fluorescence decay was calculated as a percentage of initial fluorescence measured before the addition of sodium dithionite.

$PAMPA_{lecithin}$: Stock solutions (2.5−5 μM) of each peptide were made by first dissolving the peptide in pure DMSO and then diluting the DMSO solution with PBS to achieve a concentration of 5% DMSO. The stock solution was used as starting donor well solutions for the $PAMPA_{lecithin}$ (MultiScreen-IP hydrophobic plate, cat. no. MAIPN4510/Millipore). A 1% solution of lecithin in dodecane was then added to each filter well at 5 μL per well. Immediately after adding the lipid membrane, donor solutions were added to the wells. Incubation times for all peptides were 16 h, after which the acceptor was sampled and analyzed using LC-MS. The permeability values (presented as P_e) for each peptide were obtained and compared to standards. P_e was calculated according to the following equation[38]

$$P_e = C \times \left(-\ln\left(1 - \frac{[\text{drug}]_{\text{acceptor}}}{[\text{drug}]_{\text{equilibrium}}}\right)\right)$$

$$C = \frac{V_D \times V_A}{(V_D + V_A)\text{area} \times \text{time}}$$

where V_A is the acceptor side volume, V_D is the donor side volume, area is the effective area of the membrane exposed for diffusion (cm^2), and time is the incubation time (sec).

Preparing Brush Border Membrane Vesicles: BBMVs were prepared from combined duodenum, jejunum, and upper ileum of rats by a Ca^{2+} precipitation method.[39] The intestines of five rats, 200−250 g, were rinsed with ice cold 0.9% NaCl and freed of mucous; the mucosa was scraped off the luminal surface with glass slides and put immediately into buffer containing 50 nM KCl and 10 mM Tris-HCl (pH 7.5, 4 °C), and the mixture was homogenated by Polytron (Polytron PT 1200, Kinematica AG, Switzerland). CaCl was added to a final concentration of 10 mM. The homogenate was left shaking for 30 min at 4 °C and subsequently centrifuged at 10 000 *g* for 10 min. The supernatant was then centrifuged at 48 000 *g* for 30 min, and an additional two purification steps were performed by suspending the pellet in 300 mM mannitol and 10 mM Hepes/Tris (pH 7.5) and centrifuged (24 000 *g*, 1 h). Purification of brush border membranes was assayed using the brush border membrane enzyme markers GGT, LAP, and alkaline phosphatase. During the course of these studies, enrichment in brush border membrane enzymes varied between 13-fold and 18-fold.

The enzymatic reaction was performed as follows: 2 μM stock solutions of the peptides were diluted with purified BBMV solution to a final 0.5 μM. The solution was incubated at 37 °C and sampled at time 0, 10, 20, 30, 60, and 90 min. The enzymatic reaction was stopped by adding 1:1 v/v of ice-cold acetonitrile and centrifuged (4000 *g*, 10 min) before analysis.

Conformational Analysis: Sampling the conformational space of peptides 1−18 was achieved through mixed-mode molecular dynamics (MD) simulations[40] using the AMBER force field[41] and GBSA water,[42] as implemented in the MacroModel molecular modeling package.[43] Simulations were equilibrated for 1 ns at 27 °C using a 1 fs time step and then continued for an additional 10 ns using the same temperature and time step. Representative structures were sampled every 10 ps (a total of 1000 structures) and subjected to the surface area calculations described below.

Surface Area Calculations: ZZ Vega 2.0.1 program[44] was used to calculate the surface area of each conformer. The atomic van der Waals radii used were the following: sp^2 carbons, 1.94 Å; sp^3 carbon, 1.90 Å; oxygen, 1.74 Å; nitrogen, 1.82 Å; electro-neutral hydrogen, 1.50 Å; hydrogen-bonded to oxygen, 1.10 Å; and hydrogen-bonded to nitrogen, 1.125 Å.

The polar surface area (PSA) was defined as the area occupied by nitrogen and oxygen atoms, plus the area of the hydrogen atoms attached to these heteroatoms. The positively charged N-terminus was introduced as NH_2^+. The NPSA was defined as the total surface area minus the PSA. The percentage of the surface area occupied by polar groups was also calculated.

NMR Measurements: The NMR experiments were performed on a Bruker Avance 600 MHz DMX spectrometer operating at the proton frequency of 600.13 MHz using a 5 mm selective probe equipped with a self-shielded xyz-gradient coil. The transmitter frequency was set on the HDO signal and the spectra referenced to this position at 4.77 for the water peak at 25 °C. The residual water resonance was suppressed using a Watergate sequence[445] for TOCSY[454] experiments and by low power continuous wave irradiation during the relaxation delay and the mixing time of the NOESY[23,46,47] experiments. Two-dimensional homonuclear spectra were acquired in the phase-sensitive mode with 4K complex data points in t_2 and 512 t_1 increments. The spectral width was 12 ppm and the relaxation delays were set to 1.5 and 2 s in the TOCSY and NOESY experiments, respectively. A range of temperatures between 4 and 45 °C were examined to find optimal conditions for the NMR measurements that balance minimal amide proton exchange with maximal spectrum spread. TOCSY spectra were recorded using the MLEV-17 pulse scheme for the spin lock at mixing periods of 45−75 ms with 48 scans per t_1 increment.[45,48] The NOESY experiments were investigated with mixing times ranging from 50 to 300 ms and ROESY experiments were taken with a mixing time of 150 ms.

Spectra were processed and analyzed with the XWINNMR and Viewer software packages (Bruker Analytische Messtechnik GmbH) and SPARKY (provided by Goddard, T. D. and Kneller, D. G., SPARKY 3, University of California, San Francisco) on a Silicon

Graphics Indigo2 R10000 workstation. Zero filling in the t_1 dimension and data apodization with a shifted squared sine bell window function in both dimensions was applied prior to Fourier transformation. The baseline was further corrected in the F_2 dimension with a quadratic polynomial function.

Resonance assignment was based on the TOCSY and NOESY spectra measured under identical experimental conditions.

Acknowledgment. This paper is part of the dissertation of Shmuel Hess Ph.D. We would like to thank Dr. P. Artursson for his support in PSA calculations. This work was financed in part by the Israeli Consortium of Pharmalogica.

References

(1) Borchardt, R. T.; Jeffrey, A.; Siahaan, T. J.; Gangwar, S.; Pauletti, G. M. Improvement of oral peptide bioavailability: Peptidomimetics and prodrug strategies. *Adv. Drug Delivery Rev.* **1997**, *27*, 235−256.

(2) Lipinski, C. A.; Lombardo, F.; Dominy, B. W.; Feeney, P. J. Experimental and computational approaches to estimate solubility and permeability in drug discovery and development settings. *Adv. Drug Delivery Rev.* **2001**, *46*, 3−26.

(3) Veber, D. F.; Johnson, S. R.; Cheng, H.-Y.; Smith, B. R.; Ward, K. W.; Kopple, K. D. Molecular properties that influence the oral bioavailability of drug candidates. *J. Med. Chem.* **2002**, *45*, 2615−2623.

(4) Sankararamakrishnan, R. Recognition of GPCRs by peptide ligands and membrane compartments theory: Structural studies of endogenous peptide hormones in membrane environment. *Biosci. Rep.* **2006**, *26* (2), 131−158.

(5) Drewe, J.; Fricker, G.; Vonderscher, J.; Beglinger, C. Enteral absorption of octreotide—absorption enhancement by polyoxyethylene-24-cholesterol Ether. *Br. J. Pharmacol.* **1993**, *108* (2), 298−303.

(6) Jaehde, U.; Masereeuw, R.; Deboer, A. G.; Fricker, G.; Nagelkerke, J. F.; Vonderscher, J.; Breimer, D. D. Quantification and visualization of the transport of octreotide, a somatostatin analog, across monolayers of cerebrovascular endothelial-cells. *Pharm. Res.* **1994**, *11* (3), 442−448.

(7) Hilgendorf, C.; Ahlin, G.; Seithel, A.; Artursson, P.; Ungell, A. L.; Karlsson, J. E. Expression of 36 drug transporter genes in human intestine, liver, kidney, and organotypic cell lines. *Drug Metab. Dispos.* **2007**.

(8) Lee, Y.; Sinko, P. Oral delivery of salmon calcitonin. *Adv. Drug Delivery Rev.* **2000**, *42* (3), 225−38.

(9) Knipp, G. T.; Ho, N. F.; Barsuhn, C. L.; Borchardt, R. T. Paracellular diffusion in Caco-2 cell monolayers: effect of perturbation on the transport of hydrophilic compounds that vary in charge and size. *J. Pharm. Sci.* **1997**, *86*, 1105−1110.

(10) Conradi, R. A.; Hilgers, A. R.; Ho, N. F.; Burton, P. S. The influence of peptide structure on transport across Caco-2 cells. II. Peptide bond modification which results in improved permeability. *Pharm. Res.* **1992**, *9*, 435−439.

(11) Okumu, F. W.; Pauletti, G. M.; VanderVelde, D. G.; Siahaan, T. J.; Borchardt, R. T. Effect of restricted conformational flexibility on the permeation of model hexapeptides across Caco-2 cell monolayers. *Pharm. Res.* **1997**, *14* (2), 169−175.

(12) Boguslavsky, V.; Hruby, V. J.; O'Brien, D. F.; Misicka, A.; Lipkowski, A. W. Effect of peptide conformation on membrane permeability. *J. Pept. Res.* **2003**, *61*, 287−297.

(13) Palm, K.; Stenberg, P.; Luthman, K.; Artursson, P. Polar molecular surface properties predict the intestinal absorption of drugs in humans. *Pharm. Res.* **1997**, *14* (5), 568−571.

(14) Gilon, C.; Halle, D.; Chorev, M.; Selinger, Z.; Byk, G., Backbone cyclization: A new method for conferring conformational constraint on peptides. *Biopolymers* **1991**, *31*, 745−750.

(15) Artursson, P.; Palm, K.; Luthman, K. Caco-2 monolayers in experimental and theoretical predictions of drug transport. *Adv. Drug Delivery Rev.* **2001**, *46* (1−3), 27−43.

(16) Gotoh, Y.; Kamada, N.; Momose, D. The advantages of the Uusing chamber in drug absorption studies. *J. Biomol. Screening* **2005**, *10* (5), 517−523.

(17) Rezai, T.; Yu, B.; Millhauser, G.; Jacobson, M.; Lokey, R. Testing the conformational hypothesis of passive membrane permeability using synthetic cyclic peptide diastereomers. *J. Am. Chem. Soc.* **2006**, *128* (8), 2510−1.

(18) Kerns, E. H.; Di, L.; Petusky, S.; Farris, M.; Ley, R.; Jupp, P. Combined application of parallel artificial membrane permeability assay and Caco-2 permeability assays in drug discovery. *J. Pharm. Sci.* **2004**, *93* (6), 1440−1453.

(19) Katz, M.; Ben-Shlush, I.; Kolusheva, S.; Jelinek, R. Rapid colorimetric screening of drug interaction and penetration through lipid barriers. *Pharm. Res.* **2006**, *23* (3), 580−588.

(20) Kolusheva, S.; Boyer, L.; Jelinek, R. A. colorimetric assay for rapid screening of antimicrobial peptides. *Nat. Biotechnol.* **2000**, *18*, 225−227.

(21) Su, S. F.; Amidon, G. L.; Lee, H. J. Intestinal metabolism and absorption of cholecystokinin analogs in rats. *Biochem. Biophys. Res. Commun.* **2002**, *292* (3), 632−638.

(22) Bax, A.; Davis, D. G. MLEV-17 based two-dimensional homonuclear magnetization transfer spectroscopy. *J. Magn. Reson.* **1985**, *65*, 355−360.

(23) Kumar, A.; Ernst, R. R.; Wuthrich, K. A two-dimensional nuclear Overhauser enhancement (2D NOE) experiment for the elucidation of complete proton-proton cross-relaxation networks in biological macromolecules. *Biochem. Biophys. Res. Commun.* **1980**, *95*, 1−6.

(24) Lennernas, H. Human intestinal permeability. *J. Pharm. Sci.* **1998**, *87*, 403.

(25) Pappenheimer, J. R.; Reiss, K. Z. Contribution of solvent drag through intercellular junctions to absorption of nutrients by the small intestine of the rat. *J. Membr. Biol.* **1987**, *100* (2), 123−36.

(26) Pade, V.; Stavchansky, S. Estimation of the relative contribution of the transcellular and paracellular pathway to the transport of passively absorbed drugs in the Caco-2 cell culture model. *Pharm. Res.* **1997**, *14* (9), 1210−5.

(27) Fasano, A. Modulation of intestinal permeability: An innovative method of oral drug delivery for the treatment of inherited and acquired human diseases. *Mol. Genet. Metab.* **1998**, *64* (1), 12−8.

(28) Salamat-Miller, N.; Chittchang, M.; Mitra, A. K.; Johnston, T. P. A randomly coiled, high-molecular-weight polypeptide exhibits increased paracellular diffusion in vitro and in situ relative to the highly ordered alpha-helix conformer. *Pharm. Res.* **2005**, *22* (2), 245−54.

(29) Thwaites, D. T.; Hirst, B. H.; Simmons, N. L. Passive transepithelial absorption of thyrotropin-releasing hormone (TRH) via a paracellular route in cultured intestinal and renal epithelial cell lines. *Pharm. Res.* **1993**, *10* (5), 674−81.

(30) Watson, C. J.; Rowland, M.; Warhurst, G. Functional modeling of tight junctions in intestinal cell monolayers using polyethylene glycol oligomers. *Am. J. Physiol.* **2001**, *281* (2), C388−97.

(31) Bai, J. P.; Amidon, G. L. Structural specificity of mucosal-cell transport and metabolism of peptide drugs: Implication for oral peptide drug delivery. *Pharm. Res.* **1992**, *9*, 969−978.

(32) Gilon, C.; Huenges, M.; Matha, B.; Gellerman, G.; Hornik, V.; Afargan, M.; Amitay, O.; Ziv, O.; Feller, E.; Gamliel, A.; Shohat, D.; Wanger, M.; Arad, O.; Kessler, H. A backbone-cylic, receptor 5-selective somatostatin analogue: Synthesis, bioactivity, and nuclear magnetic resonance conformational analysis. *J. Med. Chem.* **1998**, *41* (6), 919−929.

(33) Byk, G.; Halle, D.; Zeltser, I.; Bitan, G.; Selinger, Z.; Gilon, C. Synthesis and biological activity of NK-1 selective, N-backbone cyclic analogs of the C-terminal hexapeptide of substance P. *J. Med. Chem.* **1996**, *39*, 3174−3178.

(34) Afargan, M.; Janson, E. T.; Gelerman, G.; Rosenfeld, R.; Ziv, O.; et al. Novel long-acting somatostatin analog with endocrine selectivity: Potent suppression of growth hormone but not of insulin. *Endocrinology* **2001**, *142*, 477−486.

(35) Gellerman, G.; Elgavi, A.; Salitra, Y.; Kramer, M. Facile synthesis of orthogonally protected amino acid building blocks for combinatorial N-backbone cyclic peptide chemistry. *J. Pept. Res.* **2001**, *57* (4), 277−91.

(36) Falb, E.; Yechezkel, T.; Salitra, Y.; Gilon, C. In situ generation of Fmoc-amino acid chlorides using bis(trichloromethyl) carbonate and its utilization for difficult couplings in solid-phase peptide synthesis. *J. Pept. Res.* **1999**, *53* (5), 507−517.

(37) Toniolo, C. Conformationally restricted peptides through short-range cyclizations. *Int. J. Pept. Protein Res.* **1990**, *35* (4), 287−300.

(38) Wohnsland, F.; Faller, B. High-throughput permeability pH profile and high-throughput alkane/water log P with artificial membranes. *J. Med. Chem.* **2001**, *44* (6), 923−930.

(39) Peerce, B. E.; Fleming, R. Y.; Clarke, R. D. Inhibition of human intestinal brush border membrane vesicle Na^+-dependent phosphate uptake by phosphophloretin derivatives. *Biochem. Biophys. Res. Commun.* **2003**, *301* (1), 8−12.

(40) Guarnieri, F.; Still, W. C. Rapidly convergent simulation method: Mixed Monte Carlo/stochastic dynamics. *J. Comput. Chem.* **1994**, *15*, 1302.

(41) Weiner, S. J.; Kollman, P. A.; Case, D. A.; Singh, U. C.; Ghio, C. A new force feild for molecular michanical simulation of nucleic acid and proteins. *J. Am. Chem. Soc*. **1984**, *106*, 765.
(42) Hasel, W.; Hendrickson, T. F.; Still, W. C. A rapid approximation to the solvent accsessible surface area of atoms. *Tetrahedron Comput. Methodol*. **1988**, *1*, 103.
(43) Mohamadi, F.; Richards, N. G. J.; Guida, W. C.; Liskamp, R.; Lipton, M.; et al. MacroModel—An integrated software system for modeling organic and bioorganic molecules using molecular mechanics. *J. Comput. Chem.* **1990**, *11*, 440.
(44) Pedretti, A.; Villa, L.; Vistoli, G. VEGA—An open platform to develop chemo-bio-informatics applications, using plug-in architecture and script programming. *J. Comput.-Aided Mol. Des.* **2004**, *18* (3), 167−173.
(45) Piotto, M.; Saudek, V.; Sklenar, V. Gradient-tailored excitation for single-quantum NMR spectroscopy of aqueous solutions. *J. Biomol. NMR* **1992**, *2* (6), 661−5.
(46) Macura, S.; Ernst, R. R. Elucidation ofcross relaxation in liquids by two-dimensional NMR spectroscopy. *Mol. Phys.* **1980**, *41*, 95−117.
(47) Wuthrich, K. *NMR of proteines and nucleic acids*; John Wiley & Sons: New York, 1986.
(48) Sklenar, V.; Piotto, M.; Leppik, R.; Saudek, V. Gradient-tailored water supprssion for 1H-15N HSQC experiments optimized to retain full sensitivity. *J. Magn. Reson.* **1993**, *102*, 241−245.

JM070836D